RAPID COMMUNICATIONS

PHYSICAL REVIEW A VOLUME 50, NUMBER 1 JULY 1994

# Sum-frequency generation with a free-electron laser: A study of gallium phosphide

M. Barmentlo and G.W. 't Hooft
*Philips Research Laboratories, P.O. Box 80000, 5600 JA Eindhoven, The Netherlands*

E.R. Eliel, E.W.M. van der Ham, and Q.H.F. Vrehen
*Huygens Laboratory, Leiden University, P.O. Box 9504, 2300 RA Leiden, The Netherlands*

A.F.G. van der Meer and P.W. van Amersfoort
*FOM–Institute for Plasma Physics "Rijnhuizen"*
*P.O. Box 1207, 3430 BE Nieuwegein, The Netherlands*
(Received 23 February 1994)

The use of a free-electron laser (FEL) allows the study of (non)linear optical properties of materials over unsurpassed large spectral intervals. Here we report on the application of a FEL as the IR source in spectroscopic infrared-visible sum-frequency generation (SFG). Using the extremely wide tunability and the high peak power of a FEL we have studied the frequency dependence of the nonlinear susceptibility for sum-frequency generation in gallium phosphide between 20 and 32 $\mu$m in great detail. It is shown that the SFG spectrum is heavily modified by linear optical effects.

PACS number(s): 42.65.Ky, 42.62.Fi, 41.60.Cr, 78.30.Fs

Infrared-visible sum-frequency generation (SFG) is an attractive experimental method to study surfaces and interfaces that are covered with oriented molecular monolayers [1]. This is because second-order nonlinear optical techniques like SFG are surface specific when amorphous or centrosymmetric substrates are being used [1]. They allow one to gather information on the orientation of molecules on the surface or interface. All interfaces (also buried ones) that can be accessed by light may be studied with these nonlinear techniques; an ultrahigh vacuum environment is not a prerequisite. Because of these properties, first explored with optical second-harmonic generation (SHG), nonlinear optical techniques have become a relatively widely used tool for the study of surfaces and interfaces [2]. For instance, for liquid-crystal systems SHG has provided a wealth of information on the orientational alignment of the liquid-crystal molecules adsorbed on the (specifically prepared) interface [3].

For the study of oriented molecular monolayers infrared-visible sum-frequency generation is even more attractive than SHG, because it allows one to study the molecular layer in a bond specific manner with submonolayer sensitivity. When tuning the IR frequency to a vibrational resonance the response of the system is resonantly enhanced; the up-conversion process from the IR to the visible allows one to use photomultipliers to detect the generated radiation at the sum frequency. Apart from yielding molecular specificity, SFG also provides a direct probe of the effect of the interface on the bond frequencies and the orientation of specific groups within the molecule. The study of a broad range of molecular systems then necessitates a widely tunable IR laser system.

Optical parametric oscillators and amplifier systems have recently become available and this has rekindled the interest in SFG for the study of molecular layers on surfaces and interfaces [4,5]. Nowadays they operate conveniently in the 2–3.5 $\mu$m range with some systems extending to 4.5 $\mu$m. Other approaches for the generation of the required tunable IR are based on stimulated scattering in high density $H_2$ gas [6] or in a Cs vapor [7]. Right from the start of spectroscopic SFG studies, free-electron lasers (FEL's) were believed to be the ideal sources of coherent IR radiation for this type of experiment [4]. Such lasers combine high output power, extremely wide tunability, and short-pulse operation, and their output is, in terms of bandwidth, approximately transform limited. Until recently they have not been available to users. In this paper we report on a spectroscopic experiment on IR-visible SFG employing the free-electron laser for infrared experiments (FELIX), tunable between 7 and 110 $\mu$m [8,9]. In a pilot experiment we have measured the SFG spectrum of bulk gallium phosphide (GaP) between 20 and 32 $\mu$m, a wavelength interval unsurpassed in width.

Gallium phosphide has a number of attractive features that make it eminently suited for this study. For one, it shows appreciable dispersion in the IR (due to the phonon-polariton [10,11]) in a range where the free-electron laser FELIX operates conveniently [9]. This infrared active phonon-polariton is also Raman active [12–14], allowing for SFG. GaP has cubic symmetry and a zinc-blende crystal structure. So it is noncentrosymmetric and its linear optical properties are isotropic; its bulk second-order nonlinear optical properties are summarized by a single Cartesian component $\chi^{(2)}_{xyz}$ [15,16]. The latter statement is valid also near resonance, i.e., in the absence of Kleinman symmetry [17].

Frequency mixing in GaP near the phonon-polariton has been studied earlier by Faust and Henry [18]. Using a combination of a He-Ne and a far-infrared $H_2O$ laser, they were able to measure the nonlinear response of GaP at four different IR wavelengths near the *Reststrahl* at 365 $cm^{-1}$ ($\lambda = 27.2$ $\mu$m). A subsequent more extensive study helped to underpin the results of this work [19]. Both the electromagnetic and ionic character of the phonon-polariton mode contribute to the linear and the nonlinear optical response.

The IR-frequency dependence of the nonlinear suscepti-

 

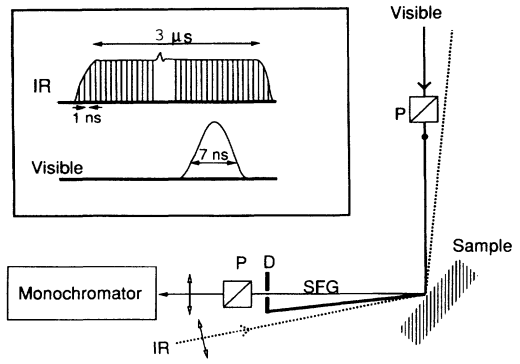


FIG. 1. Reflection setup for infrared-visible sum-frequency generation in bulk materials or on interfaces. The generated light at the sum frequency emerges from the interface under a small angle relative to the reflected visible beam. The reflected visible beam is intercepted by a diaphragm. Spatial and spectral filtering are used to extract the SFG signal. The inset shows the timing structure of the infrared and visible laser pulses.

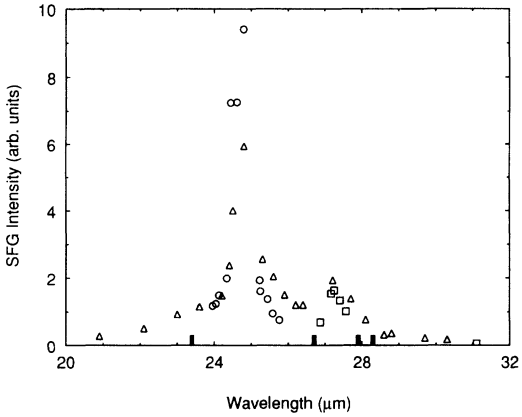


FIG. 2. Experimental SFG spectrum of GaP normalized to the infrared and visible laser powers. The various data points represent different experimental runs. The bars indicate the wavelengths where measurements have been performed earlier [19].

bility for SFG can be written as [18]

$$\chi^{(2)}(\omega_{SFG}=\omega_{IR}+\omega_V)=A_0\left[1+\frac{C\omega_0^2}{\omega_0^2-\omega_{IR}^2-i\omega_{IR}\Gamma}\right]. \tag{1}$$

Here $\omega_0=\omega_{TO}$ is the frequency of the transverse optical phonon, $\Gamma$ the damping rate of the phonon ($\Gamma\approx 0.01\omega_0$ at room temperature), $C$ a constant, found to be $C=-0.53\pm 0.03$, and $A_0$ a proportionality constant; $\omega_V$ and $\omega_{IR}$ are the input visible and IR frequencies, and $\omega_{SFG}$ is the sum frequency. The interference of the two terms in the expression for $\chi^{(2)}$ [see Eq. (1)] leads to a sharp peak in $|\chi^{(2)}|$ at $\omega_{IR}=\omega_0$ ($\lambda=27.2$ $\mu$m) and a minimum at $\lambda=40$ $\mu$m corresponding to the point where $\omega_{IR}=\omega_0\sqrt{C+1}$. The experimental data obtained by Faust and Henry were—although limited to four points—in satisfying agreement with this model.

In our experiment the $p$-polarized beam of the FELIX free-electron laser (diameter $\approx 4$ mm) is mixed with the nearly counterpropagating $s$-polarized beam (diameter $\approx$ 8 mm) of a pulsed frequency-doubled neodymium-doped yttrium aluminum garnet (Nd:YAG) laser in a [001]-cut single crystal of GaP oriented with its [001] axis bisecting the angle subtended by the input beams, and its [100] axis at an angle of $\pi/4$ relative to the input plane. A reflection setup is used (see Fig. 1), particularly appropriate for interfacial studies [4], and the $p$-polarized SFG signal is measured. Spatial, spectral, and polarization filtering is used to extract the SFG signal. The forward generated SFG radiation is absorbed in the bulk of the GaP crystal. The detected radiation at the sum frequency is generated in backreflection by a thin layer at the air-GaP interface, the thickness of which ($\approx$12 nm) is determined by phase-matching considerations (see below).

FELIX generates a long ($\approx 3$ $\mu$s) train of short (1–10 ps) energetic ($\approx 2$ $\mu$J) micropulses at a repetition rate of 1 GHz. Temporal overlap with the visible radiation (pulse energy $\approx$ 2.5 mJ) is easily achieved in the present setup as the visible laser yields a pulse ($\approx$ 7 ns), long compared to the duration and separation of the micropulses of FELIX (see the inset of Fig. 1). Both FELIX and the visible laser operate at a repetition rate of 5 Hz. Note that in this setup only a small fraction of the total available visible and FELIX energy is being used (0.5% and 0.2%, respectively).

The results of the SFG experiment on GaP are shown in Fig. 2. One strong ($\lambda\approx 24.8$ $\mu$m, $\nu\approx 403$ cm$^{-1}$) and one weaker ($\lambda\approx 27.2$ $\mu$m, $\nu\approx 367$ cm$^{-1}$) resonance can be distinguished. Also indicated in Fig. 2 are the four wavelengths (23.4, 26.7, 27.9, and 28.3 $\mu$m) of Faust *et al.* [19] that fall in the wavelength region that is studied here. Our data show that the nonlinear response exhibits large variations in between these data points. The signal strength at the peak of Fig. 2 corresponds to roughly $2\times 10^4$ photons/micropulse.

It is tempting to attribute the two observed peaks to the LO and TO zone-center optical phonons in GaP (402.8 and 367 cm$^{-1}$, respectively) [14]. This would seem to contradict the model of Eq. (1). In addition to the expected resonant response at the frequency of the TO phonon, we observe an even larger response at the frequency of the LO phonon. The discrepancy is caused by the fact that the experimental signal strength is determined not only by the nonlinear but also by the linear optical properties of GaP, both of which show large variations in the wavelength interval of interest. The linear optical properties affect the Fresnel transmission and reflection coefficients of the incident and generated fields across the air-GaP interface on the one hand, and the thickness of the interaction layer on the other. For instance, the presence of a band gap in the dispersion of the phonon-polariton results in values of the refractive index $n<1$ and a large extinction coefficient $\kappa$ in the band-gap region $\omega_{TO}<\omega<\omega_{LO}$. As a result, the reflectivity is very high in this spectral region and the IR radiation hardly couples into the material. Basically, one has total external reflection in the band-gap region. However, the evanescent field at frequency $\omega_{IR}$ penetrates the material, allowing SFG to occur.

The thickness of the layer ($\approx$ 12 nm) at the air-GaP interface from which the detected radiation emanates is determined by the coherence length for the nonlinear conversion process $l_c=[|\Delta\mathbf{k}'|^2+(\alpha/2)^2]^{-1/2}$. The first factor in this expression represents the mismatch between the wave vectors $\mathbf{k}'$ inside the material $|\Delta\mathbf{k}'|=|\mathbf{k}'_{SFG}-\mathbf{k}'_V-\mathbf{k}'_{IR}|$. In the

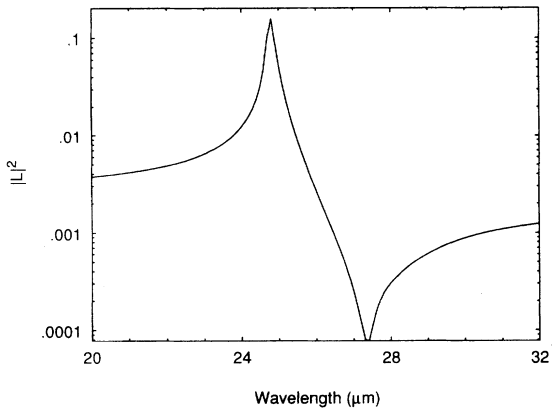


FIG. 3. The Fresnel coupling coefficient $|L|^2$ for the air-GaP interface for the experimental situation of Fig. 2.

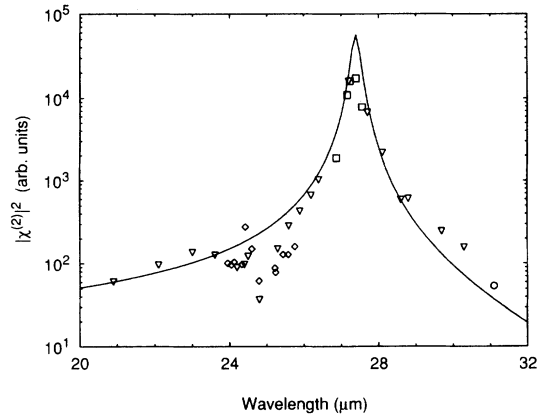


FIG. 4. Wavelength dependence of $|\chi^{(2)}|^2$ for sum-frequency generation in GaP as deduced from the experimental results of Fig. 2 upon correction for the strong wavelength dependence of the Fresnel coupling coefficients. The various data points represent different experimental runs. The solid curve shows the results of a simple model for the nonlinear susceptibility for SFG in GaP as given in Eq. (1).

reflection setup used in the present experiment $|\Delta\mathbf{k}'|\approx 2|\mathbf{k}'_V| = 83\ \mu\text{m}^{-1}$ (the wave vectors $\mathbf{k}'_{SFG}$ and $\mathbf{k}'_V$ are almost antiparallel inside the crystal), largely insensitive to the dispersion in $\mathbf{k}'_{IR}$ (as $|\mathbf{k}'_{IR}| << |\mathbf{k}'_V|$). The second factor in the expression for the coherence length results from absorption. Although the absorption coefficient for the IR radiation shows large dispersion, its peak value ($\alpha \approx 5\ \mu\text{m}^{-1}$) is much smaller than the value of $|\Delta\mathbf{k}'|$. So the coherence length for the nonlinear conversion process is dominated by the effects of wave-vector mismatch and the variation of the absorption coefficient of the IR does not come into play. In the present discussion the variation of $l_c$ with wavelength is henceforth neglected.

As the coherence length can be assumed to be constant the nonlinear response can now be simply calculated using the values of the electric fields at the various frequencies just inside the material, connected to those outside the material by the appropriate Fresnel coefficients [20]. Again, for the infrared radiation these coefficients are strongly wavelength dependent and so is the magnitude of the electric field at frequency $\omega_{IR}$ inside the sample. The effects of the Fresnel coupling across the air-GaP interface on the SFG intensity are contained in the factor $|L|^2$, the wavelength dependence of which is shown in Fig. 3. Note that $|L|^2$ varies over more than three orders of magnitude between $\omega_{LO}$ and $\omega_{TO}$. Near $\omega_{LO}$ the IR field is well coupled into the medium, in contrast to the frequency range around $\omega_{TO}$. The Fresnel coefficients thus cause a major skewing of the SFG spectrum.

Figure 4 shows the SFG spectrum of GaP after correction for the Fresnel coupling, using the values for $|L|^2$ as shown in Fig. 3. The corrected spectrum shows a single large resonance around $\omega_{TO}$ in line with what is to be expected. The additional (and largest) peak in the experimental SFG spectrum represents nearly resonant SFG strongly enhanced by simple linear optical effects. Also included in Fig. 4 are the results of the model of Eq. (1). Good agreement is found between this model and our detailed experimental results. Note that our ability to fully resolve the sharp peak in $|\chi^{(2)}|^2$ is limited by the finite bandwidth of FELIX ($\Delta\lambda/\lambda \approx 0.01$).

The peak value of the nonlinear susceptibility shown in Fig. 4 corresponds to a value, as derived from the experiment, for the effective surface susceptibility $|\chi^{(s)}_{eff}| \simeq 7\times 10^{-18}$ m$^2$/V, using standard expressions for the signal strength in surface second-order processes [1,20]. Using $\chi^{(s)}_{eff} \simeq l_c\chi^{(2)}$ we have $|\chi^{(2)}| \simeq 6\times 10^{-10}$ m/V for the bulk susceptibility of GaP at the phonon-polariton resonance.

The present experiment has a detection limit for $|\chi^{(s)}_{eff}|$ of the order of $7\times 10^{-19}$ m$^2$/V, a typical monolayer value [1]. A large improvement in the detectivity is expected when a visible laser system is used that has much better temporal overlap with the FELIX free-electron laser as compared to the system that has been used. Work along these lines is in progress.

To summarize, by employing the FELIX free-electron laser in combination with a pulsed visible laser system we have been able to explore the SFG spectrum of bulk GaP in fine detail over a very large spectral range. The results are in good agreement with earlier data on frequency mixing in GaP where the nonlinear response was measured at a small number of IR wavelengths only. The experimental sum-frequency spectrum is determined by both the linear and the nonlinear optical response, both of which are resonantly enhanced around the phonon-polariton. The large increase in the value of $\chi^{(2)}$ is partially compensated by a strong reduction of the IR field inside the material in the phonon-polariton band-gap region. The different wavelength dependence of these two effects causes a double-peaked SFG spectrum for a single resonance. It is noteworthy that, although the IR cannot propagate in the material in the band-gap region, the evanescent field is sufficiently large to generate easily detectable radiation at the sum frequency. In this study we have fully employed the wide tunability and large peak powers of the FELIX free-electron laser, showing that free-electron lasers are eminently suited for nonlinear optical studies of materials over very wide spectral ranges. The ability to probe the nonlinear optical response at arbitrary infrared wavelengths makes FEL-based SFG a powerful spectro-

scopic tool with many applications in solid-state physics, interface physics, and chemistry.

We gratefully acknowledge R.J. Hollering for stimulating discussions. Part of the present work is part of the research program of the "Stichting voor Fundamenteel Onderzoek der Materie (FOM)" and of the Technology Foundation, and was made possible by financial support from the "Nederlandse Organisatie voor Wetenschappelijk Onderzoek (NWO)."

[1] See, for example, Y.R. Shen, Nature (London) **337**, 519 (1989).

[2] M. Buck, Appl. Phys. A **55**, 395 (1992).

[3] M. Barmentlo, F.R. Hoekstra, N.P. Willard, and R.W.J. Hollering, Phys. Rev. A **43**, 5740 (1991); M. Barmentlo, R.W.J. Hollering, and N.A.J.M. van Aerle, *ibid.* **46**, 4490 (1992); M. Barmentlo and Q.H.F. Vrehen, Chem. Phys. Lett. **209**, 347 (1993).

[4] X.D. Zhu, H. Suhr, and Y.R. Shen, Phys. Rev. B **35**, 3047 (1987).

[5] Q. Du, R. Superfine, E. Freysz, and Y.R. Shen, Phys. Rev. Lett. **70**, 2313 (1993).

[6] T.H. Ong, P.B. Davies, and C.D. Bain, Langmuir **9**, 1836 (1993).

[7] A.L. Harris, C.E.D. Chidsey, N.J. Levinos, and D.N. Loiacono, Chem. Phys. Lett. **141**, 350 (1987).

[8] The first spectroscopic IR-visible SFG experiment with a FEL was reported by M. Barmentlo, G.W. 't Hooft, R.W.J. Hollering, E.R. Eliel, Q.H.F. Vrehen, A.F.G. van der Meer, and P.W. van Amersfoort (unpublished); M. Barmentlo, Ph.D. thesis, Leiden, 1993.

[9] R.J. Bakker, C.A.J. van der Geer, D.A. Jaroszynski, A.F.G. van der Meer, D. Oepts, and P.W. van Amersfoort, J. Appl. Phys. **74**, 1501 (1993).

[10] D.A. Kleinman and W.G. Spitzer, Phys. Rev. **118**, 110 (1960).

[11] A.S. Barker, Jr., Phys. Rev. **165**, 917 (1968).

[12] C.H. Henry and J.J. Hopfield, Phys. Rev. Lett. **15**, 964 (1965).

[13] A.S. Barker, Jr. and R. Loudon, Rev. Mod. Phys. **44**, 18 (1972).

[14] R.M. Hoff and J.C. Irwin, Can. J. Phys. **51**, 63 (1973).

[15] R.W. Boyd, *Nonlinear Optics* (Academic Press, San Diego, 1992).

[16] M. Schubert and B. Wilhelmi, *Nonlinear Optics and Quantum Electronics* (Wiley, New York, 1986).

[17] D.A. Kleinman, Phys. Rev. **126**, 1977 (1962).

[18] W.L. Faust and C.H. Henry, Phys. Rev. Lett. **17**, 1265 (1966).

[19] W.L. Faust, C.H. Henry, and R.H. Eick, Phys. Rev. **173**, 781 (1968).

[20] See, e.g., Y.R. Shen, Surf. Sci. **299**, 551 (1994).